

The GBT Precision Pointing System

Donald C. Wells¹

National Radio Astronomy Observatory
Charlottesville, VA
dwells@nrao.edu
804-296-0277

NOTE

This memo is *not* identical to the draft version which was distributed to 18 people on August 5; I recommend that copies of the draft be discarded. See the "Special Note" (p. iii) for a summary of the changes, as well as an overview of the parts which are not completed.

September 25, 1992

¹with VLBA Correlator project, temporarily assigned to GBT during July 1992.

Contents

Special Note	iii
Preface	iv
1 Technical Strategy	1
1.1 “Outside-In” versus “Inside-Out”	2
1.2 Pointing Information Sources	2
1.2.1 Laser Ranging	2
1.2.2 Autocollimator	8
1.2.3 Inclinator	9
1.2.4 Temperature Sensors	9
1.2.5 Refraction Models & Sensors	10
1.2.6 Wind Sensors	15
1.2.7 M&C Motion Plan	15
1.2.8 Radio-Source Observations	16
1.3 Analysis Techniques	16
1.3.1 Structural Modelling	17
1.3.2 The “Rubber-Sheet” Function	19
1.3.3 Bootstrapping Retroreflector Coordinates	19
1.3.4 Offline Analysis	21
1.3.5 Vibration Modes and Pointing	22
1.3.6 Adaptive Measurement Techniques	23
1.3.7 Potential of Neural Nets	24
1.4 Surface Control	24
1.4.1 Open-Loop, Closed-Loop	24
1.4.2 Surface Servo	25
1.4.3 The “Mouse”	25
1.4.4 Initial Adjustment of the Panels	26
1.4.5 Holographic Measurements	26
1.4.6 Beam Direction and Beam Shape	27
1.5 Destinations for Pointing Information	27

2	Interfaces	28
2.1	Interface to M&C	28
2.1.1	Asynchronous RT Processes	29
2.2	Interface to Laser Ranging	29
2.2.1	Implementation Details	30
2.2.2	Range-rate Requirement	30
2.3	Interface to Active Surface	31
2.4	Interface to Autocollimator	31
2.5	Interface(s) to Environmental Sensors	32
2.6	Interface to Operator & User	32
3	Component Choices	33
3.1	Hardware Choice	33
3.2	OS Choice	33
3.3	Language Choice(s)	33
4	Development Plan	34
4.1	Staffing	34
4.1.1	Understudy Concept	34
4.1.2	Mathematics & Engineering Support	34
4.2	Budget	34
4.2.1	Hardware Components	34
4.2.2	Software Components	34
4.3	Schedule for Precision Pointing Project	35
4.3.1	Phasing	36
4.3.2	Contingency	36
4.3.3	Issues and Possibilities	36
4.3.4	Technical TBDs	37
A	Acknowledgements	39
	Bibliography	42

Special Note

I spent much of July and the first week of August working on this GBT memo. Readers will notice that it is incomplete. I have been urged by various people to distribute it anyway, rather than taking time from the VLBA project to improve it. I have made some changes:

- figure 1.1 was added.
- a footnote was added.
- minor typographic, nomenclature and grammar corrections were applied.

As a result of a number of discussions with various people, I have concluded that:

- Probably we will not need to compute structural models in near-real-time, as discussed in section 1.3.1 (p.17) because grids of the deflections due to gravity and wind-loading can be calculated off-line as a function of elevation and relative azimuth. The problem is linear, so the tabulated deflections due to the two effects can be summed with appropriate weights. Temperature varies slowly, so deflections due to it can be calculated more slowly. This technique will significantly reduce the computing requirements.
- The “mouse” discussed in Section 1.4.3 will not be needed because RSi will give us a copy of the digital panel maps which they will produce in the Sterling factory as the panels are being manufactured. A modest set of measurements will confirm the validity of the maps.
- Work on anomalous refraction can be deferred, because it will not be a problem under good winter conditions, and high-frequency VLBI work will be able to mostly correct for it with self-cal.
- The project concept is modular, so temperature and vibration modelling can be deferred, and added as time permits.
- We should defer procurement of a 10 μ m camera until after the GBT is built, when we can borrow one and evaluate whether the project should buy one or more of them.
- We will probably use the rangefinders to do a series of pointing and modelling experiments with one or more existing NRAO telescopes during 1993. Structural models exist for both the VLBA telescopes and the 140 Foot.

Don Wells
September 24, 1992

Preface

*“Make no little plans;
they have no magic to stir men’s blood.”¹*

I have agreed to organize and lead the project which will produce pointing software for the GBT. Recently Geoff Croes and Bob Hall asked me to prepare a planning document for this software project. They, and Jay Lockman, have emphasized to me that the plan should define as many of the system interfaces as possible, so that development of other GBT systems will not be inhibited by uncertainties about the pointing software. I agreed to prepare this first draft during the month of July 1992, while the VLBA Correlator is being shipped to Socorro. I expect to be able to join the GBT construction project team on January 1, 1993.

The plan I am proposing in this document has a number of complicated and unprecedented features. There are uncertainties associated with several of its elements, i.e., it is a *research* project to some extent. This is right and proper if our goal is to produce the highest performance pointing system which is possible. *I insist that that should be our goal.* We should strive to minimize the overhead of pointing calibrations for centimeter-wave observations and we should strive to “push the envelope” for higher frequency operations.² Even though Green Bank is not an optimal site for millimeter observations, the 8000 m² collecting area of the GBT will have tremendous potential on cold winter nights. Efficiency and automation and *precision pointing* will be critical for effective utilization of those nights. It is this important strategic goal that has motivated me to dare to propose a plan based on unprecedented technical approaches.

¹Daniel Hudson Burnham 1846-1912

²[Sei89] discusses the scientific justifications for high frequency operation of the GBT. On p.3 they are summarized as: (1) unequalled capability at 3 mm with more than 70 m diameter, (2) importance of VLBI at 43 and 90 GHz and (3) “CO more sensitive per nucleon than H I”.

Chapter 1

Technical Strategy

Strategic considerations for pointing the GBT have been discussed in a number of documents [AUI89, Fin89, Pay90, Bro90a, Con92]; this memo is one more in the series. The special aspect of this planning memo is that it discusses a *software*-based strategy to complement the (primarily) hardware-based strategies which have been discussed previously.

In [Pay92], John Payne distinguished two classes of pointing errors, “repeatable” and “non-repeatable”. The repeatable class includes problems like collimation, azimuth track irregularities and gravity loading. The non-repeatable class includes thermal effects in the alidade structure (believed to be the largest error source in the GBT), wind and thermal changes in the main reflector, wind and thermal changes of lateral position of the subreflector, thermal change of the axial position of the subreflector, wind and thermal changes of the tilt of the subreflector, and anomalous refraction problems. Payne expects that the use of autocollimator, inclinometer and rangefinder sensors can enable correction of many of the non-repeatable errors.

Several of these non-repeatable pointing errors can be *computed* if sufficiently detailed wind and thermal data are available. Others are not computable: differential thermal effects on scales smaller than spacing of the temperature sensors in the structure, wind turbulence noise at frequencies greater than perhaps 0.2 Hz and—ultimately most important—changes of refraction for which we have neither computable models nor sensors. In this plan I propose that we utilize both a rich array of sensors and a set of numerical models, and that we *compute* the precision pointing of the GBT from the models while continuously confirming their validity with freshly-acquired sensor data.

A key strategic concept of this plan is the use of numerically-intensive CAD tools to model the flexure and distortions of the telescope structure *in real-time*. Such an approach is now feasible, in an era when the price-performance ratio of computers is approximately doubling each year. I propose to utilize high-precision laser ranging data plus autocollimator angle data to confirm and refine the pointing errors predicted by numerical structural models. Thermal distortions will be computed from detailed temperature measurements, wind-loading distortions from wind and pressure sensors. Thus, the Precision Pointing System [PPS] will be mainly “open-loop” (computing corrections from numerical models) on short timescales, but will be closed-loop on longer timescales as the data are used to evolve the numerical models.

The discussion which follows concentrates on pointing for the Gregorian optics, because the GBT will be constructed with sufficient precision as to be nearly perfect for the low frequencies which will be used at the prime focus. The strategic approach proposed here will also be applied to the prime focus.

1.1 “Outside-In” versus “Inside-Out”

In [Con92], Jim Condon described the use of a 2-D Fourier series for representing pointing errors measured from observations of radio sources. His approach is an elegant refinement of the classical, well-proven strategy for telescope pointing: the telescope is treated mostly as a black box, and pointing corrections are derived solely from observations of sources in the sky. The goal of this strategy is not so much to understand the causes of the pointing errors as it is to produce an efficient numerical map of the repeatable error components, plus perhaps some corrections for some non-repeatable error components. I call this the “outside-in” strategy.

Laser rangefinders plus structural models will enable the GBT project to adopt a new (and unprecedented) strategy: the black box can be opened up and we can analyze its interior in detail, with the goal of understanding the physical behavior of the machine. The end-result will be a numerical map which not only will have improved resolution and precision, but which will also include modelling of several types of non-repeatable errors. In particular, thermal effects can be computed by injecting temperature data into the structural models. The detailed understanding of all of the physical effects is likely to lead to a superior diagnostic ability when tracing faults like loose or broken elements, bearing misbehavior, particular sources of thermal problems, etc. A special advantage of this technique will be its ability to cope with structural vibrations, which may turn out to be a serious problem for the GBT. The structural models will tell us the shape (eigenvectors) of the various modes (eigenvalues), and we can implement phase-locked loops to track the primary modes in software. The structural model approach will also provide open-loop servoing of the active-surface, reducing the burden of laser rangefinders for surface control. For all of these reasons, *I strongly recommend that the GBT adopt this “inside-out” strategy*, rather than the traditional “outside-in” strategy.

1.2 Pointing Information Sources

In this section I discuss the various sensors which are relevant to pointing, plus pointing-related information entering the pointing system from the M&C system.

1.2.1 Laser Ranging

The laser ranging instruments which have been developed at Green Bank during the past two years are able to measure ranges of order 100 meters with errors of about 50 microns RMS. These instruments [PP90, PPB92] are *the* critical component of the “inside-out” strategy for precision pointing of the GBT. Figure 8 of [Pay92] is an excellent schematic of the proposed configuration of the rangefinders in the GBT.

1.2. POINTING INFORMATION SOURCES

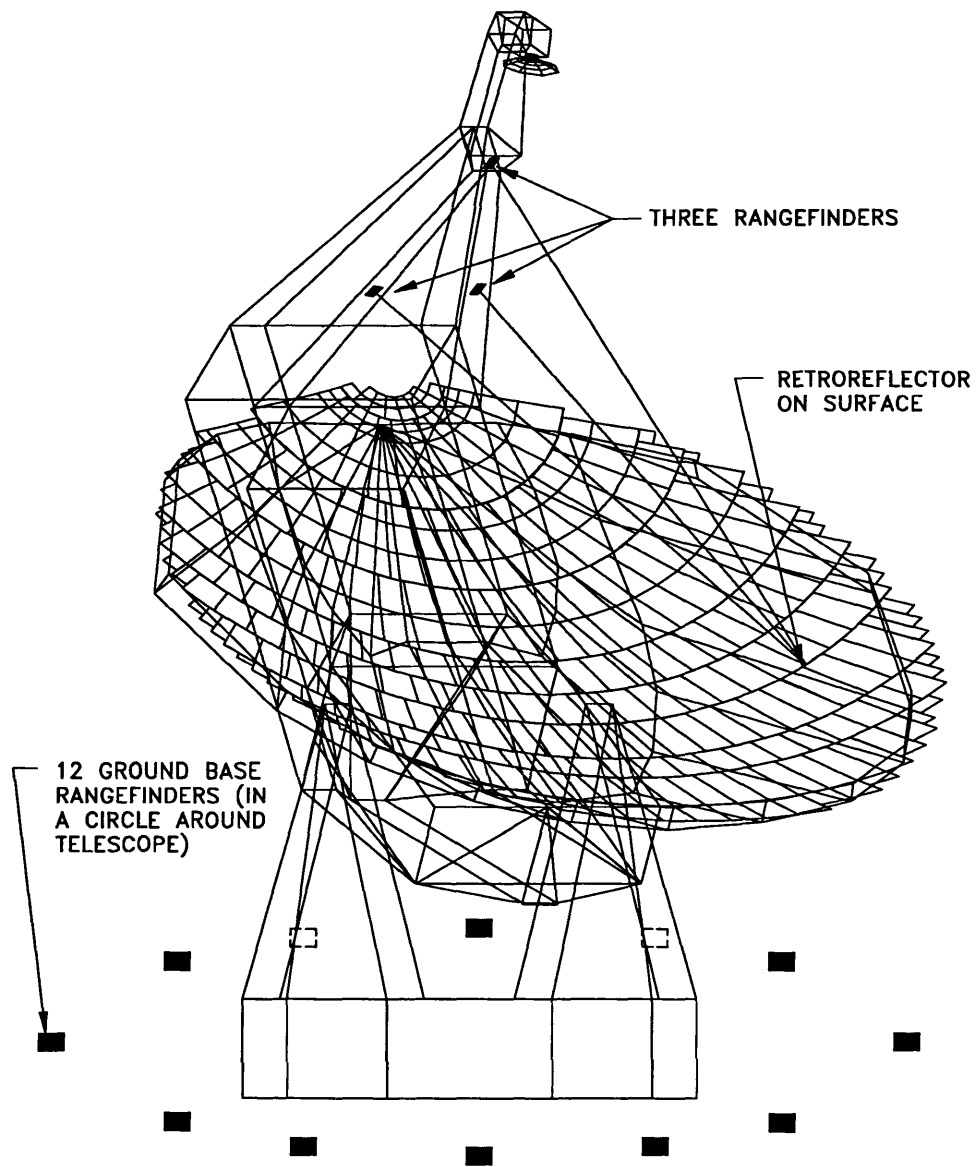


Figure 1.1: Rangefinders on Piers and on the Feed Arm

The laser beams and the optical elements will be in the open air, subject to blockage by condensation. Anecdotal remarks suggest that fog will not be a problem, as the SNR of the lasers is high and the attenuation is modest, but actual condensation on the optics will cause severe attenuation. Probably we can actively heat the most important optical elements, but the basic condensation problem implies that the PPS cannot *depend* on the rangefinders—it must degrade gracefully as rangefinder data becomes unavailable.

The zero point of the laser rangefinders as manufactured is arbitrary. Payne has recommended [Pay91] that an H-P rangefinder be procured to calibrate a test range which would be used to calibrate the zero points of the NRAO rangefinders. I believe that regression analysis would be able to determine these zero points from redundant measurements, but removing these variables by calibration would free up statistical weight in the datasets which could be applied to the remaining variables.

From Ground to Alidade

Laser rangefinders mounted on piers around the GBT will be able to measure distances to retroreflectors mounted on all parts of the alidade structure. Ranges to reflectors mounted near the four trucks will indicate the azimuth of the base of the telescope, which should agree with the azimuth encoder. Ranges to reflectors at several heights on the four main legs of the alidade will enable detection of thermal distortions. Finally, reflectors mounted near the bearings of the elevation axle will enable determination of the orientation of that axle independent of other sensors (autocollimator, inclinometers and encoders). The major source of thermal distortion and the most important vibration modes of the GBT will be measureable with this rangefinder data.

From Ground to Dish

Consider a laser rangefinder measuring from a pier to a retro-reflector at the edge of the dish (Figure 1.2). The radius from the elevation axle is ≈ 50 meters and the RMS of the range measurement is ≈ 50 microns, so the angular position of the dish is measureable to $\approx 10^{-6}$ radians, i.e. to **0.2 arcsec RMS** for single measurements. The noise of the laser ranges appears to normally distributed, so a least squares solution for the angular position may have an RMS as low as 0.1 arcsec.

Notice that two rangefinders measuring opposite sides of the dish can determine the direction of the dish independent of the alidade structure. Also notice that if atmospheric effects scale the ranges by some unknown factor the angles will be conserved [vH90]. These basic intuitive ideas make me optimistic that the laser rangefinders will ultimately enable us to eliminate the telescope itself as a source of pointing error.

There are, of course, a number of important details which are ignored in the two paragraphs above:

- Inhomogeneities of the atmosphere around the telescope produce fluctuations of the index of refraction, which imply fluctuations of range measurements. Gradients of index can produce distortions of the inferred geometry of the telescope.

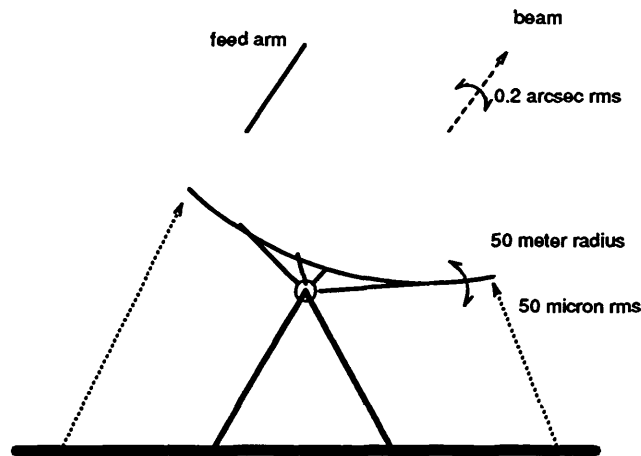


Figure 1.2: Intuitive Concept of Rangefinders & Dish Orientation

- The direction of the radio beam is primarily determined by the direction of the dish, but the dish may have the wrong shape or the feed arm may be deflected from its nominal position.
- The locations of the rangefinders and retroreflectors relative to the telescope are not known a priori; pointing information cannot be derived from them until the geometry has been calibrated.
- It would not be prudent to use raw laser ranging data in a closed-loop computation of pointing corrections because the system would not degrade gracefully under component failures, and because the servo bandwidth would then depend on the (limited) laser measurement rate.
- It is improbable that the GBT will point to 0.1 arcsec *on the sky*, even if the laser permits us to point the structure with that precision, due to non-repeatable, uncomputable and uncalibratable changes of the component of refraction due to water vapor. Such changes are likely to be the ultimate limitation for GBT pointing.

We will need to measure the retroreflectors at the edge of the dish with lasers at a variety of positions. The current plan is to fabricate some sort of assembly to hold a number of reflectors at the same radius from a point; I call such an object a “retro-sphere”. A retrosphere would be manufactured in the shop such that the centroid of the sphere will be calculable from ranges to individual retroreflectors on the sphere. The retrospheres should be warmed to assure that they will be available as much as possible.

F. Schwab has recently been calculating pointing errors for various distributions of rangefinders and retrospheres. Figure 1.3 was supplied by Schwab. It shows the GBT at 50 degrees elevation, with 12 retrospheres around the rim of the dish and 16 rangefinders in a ring 85 meters from the pintle bearing. Of the 192 possible paths, 82 are active

(unobstructed) in this figure. The scales are in meters. This type of configuration (a “truss” of laser beams) determines the orientation of the dish relative to the piers with great redundancy and statistical weight.¹

From Dish to Feed Arm

Three rangefinders will be mounted in a large triangle on the feed arm in order to triangulate on the 2213 retroreflectors attached to the panel actuators. These three rangefinders will also triangulate on the retrospheres mounted around the edge of the dish. This implies that the shape of the surface will be measured—in detail—relative to the retrospheres, whose locations will be known relative to the piers in the ground.² The position of the triangle of rangefinders on the feed arm will also be determined by this process.

From Feed Arm to Subreflector

Three (or six?) retroreflectors mounted around the edge of the subreflector will define its position and orientation in the telescope. Probably the three rangefinders mounted on the feed arm will be able to “see” the subreflector; if not, three more rangefinders can be mounted on the turret to measure the subreflector position relative to the rangefinders on the feed arm. The objective is to measure the subreflector position in coordinates which are traceable to the piers.

From Feed Arm to Turret

If the three rangefinders on the feed arm are able to “see” the subreflector and the top of the Turret, we might be able to mount three retroreflectors around the focal point to define its location. Alternatively, we could install three rangefinders on the turret. In any case, we will need to define a coordinate system associated with the feed room and relate it to the feed arm so that we can calculate where on the sky any point on the turret is mapped at any moment.

Initial Calibration of Geometry

If one of the laser rangefinders on the piers around the telescope has a TV camera we can use simple astrometry on bright stars to determine the azimuth and zenith of the laser ranging system, probably with an error of less than 10 arcsec. This should permit us to point the GBT at the moment of first light to about that precision.

¹Schwab’s analysis predicts RMS pointing of ≈ 1.5 arcsec. Several people have asked me about the discrepancy between this number and the 0.2 arcsec estimate I gave above. The answer is that Schwab’s analysis is concerned with the orientation of the triangle of rangefinders in the feed arm, and uses the retrospheres only to transfer coordinates from the piers to the arm—the retrospheres are not assumed to be a part of the dish.

²In addition, the rangefinders on the piers will be able to measure changes of the backup structure “shape” relative to the retrospheres; therefore, after the geometry is calibrated the shape of the dish can also be inferred from measurements of the backup structure.

1.2. POINTING INFORMATION SOURCES

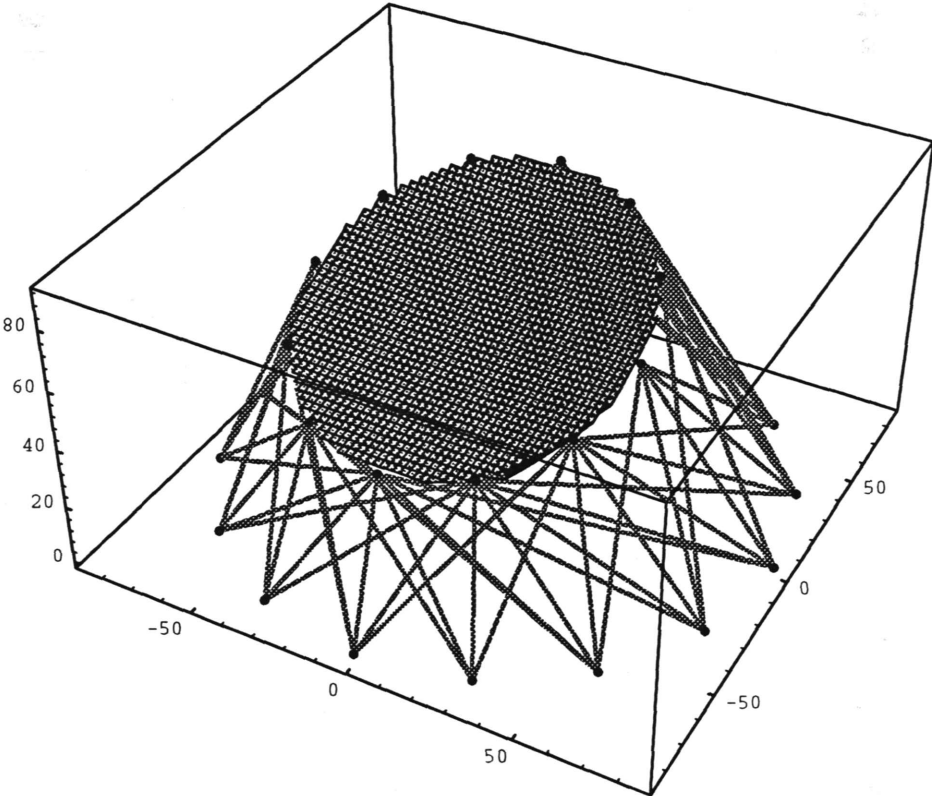


Figure 1.3: 16 Rangefinders, 12 Retrospheres, 82 Paths

Potential of Acoustic Thermometry

A range measured with a laser rangefinder is dependent on the average index of refraction along the path, and the index varies with air temperature. Fluctuations of the index due to temperature are observed, and are a cause for concern [Hog90]. The major effects are expected to occur on sunny days. At night the structure may cool by radiation to a temperature below ambient and air cooled by conduction may flow over the dish, and affect rangefinder measurements. There will be a gradient of temperature from the ground up to highest part of the GBT, about one degree C total.

Payne and Parker tested an experimental acoustic time-of-flight instrument recently. [PPMR92] It measures the average temperature along a path. Variations of the temperature are closely correlated with apparent variations of range seen with a rangefinder on the same path. This work looks very promising, and implies that we may be able to sense the atmospheric temperature distribution along many different paths around the telescope. For example, we might install an acoustic transmitter on each laser instrument and a microphone on each retrosphere, so that we could simultaneously measure the average temperature above and below the dish along the majority of our most important paths.

Air Temperature Sensors?

It would be interesting to know the power spectrum of air temperature variations at a point in addition to measuring its integral along a line with acoustic thermometry. We could install air temperature sensors on towers around the telescope to sense the upstream air, perhaps six towers, perhaps 30 m (50?) high, perhaps 150 m (200?) radius from telescope, perhaps 10 sensors per tower. Sensors near ground level would give surface air temperature, which would be used to calculate laser ranging basic index of refraction and the atmospheric refraction. The temperature sensors at various heights provide a check on the nominal atmospheric lapse rate (-0.0065 °C/m), which will be used to calculate the variation of index of refraction (laser ranging scale factor) with height. At this time I do not think we really need this level of sensing of air temperature.

1.2.2 Autocollimator

The autocollimator system [Bro90a] will measure angular rotations of the upper portions of the alidade structure relative to its base. It will be a source of information for the PPS which will be independent of the laser ranging system, a source which is not vulnerable to extremes of condensation. The rotation measures will include the effects of wind loading and thermal distortions of the alidade structure, and they will also see twisting of the alidade due to irregularities of the azimuth track.

The lowest frequency (most important) vibrational modes of the GBT will be the lateral and torsional modes of the tines of the alidade fork; the autocollimator will *directly* measure the angular displacements produced by these modes. The resolution is ≈ 0.1 arcsec with a bandwidth of ≈ 1 Hz. See Figure 26 on p.80 of [FvH72] for illustrations of the vibration modes of an alidade.

1.2.3 Inclinometer

Inclinometers have been installed at the ends of the elevation axles of several telescopes to detect the same rotations which the autocollimator system will detect. Inclinometers are relatively inexpensive and they are sensitive; their wide bandwidth (≈ 10 Hz) probably implies that they will be excellent detectors of the higher vibration modes of the structure.³ They will also confirm the autocollimator and laser results. I recommend that the GBT seriously consider procuring two inclinometers.

1.2.4 Temperature Sensors

The thermal expansion coefficient for A36 steel is $11.7 \mu\text{m}^{-1}\text{C}^{-1}$. “11.7” is the average value between 0°C and 100°C ; from 0 to 200°C the coefficient increases by 4%. [Kin92b] A one degree change of ambient temperature will increase the overall height of the GBT by about $1500\mu\text{m}$ (1.5 mm). The standard atmospheric lapse rate implies that the top of the GBT will be about 1°C cooler than the base. The $50\mu\text{m}$ RMS noise of the laser rangefinders implies that we will easily detect the effects of an overall temperature change of 0.1°C . A good overview of thermal problems in antennas is in memo [Lam92b]. These various considerations all imply that thermal effects will be a major cause of pointing difficulties for the GBT. We will need to install temperature sensors throughout the structure.

Thermocouples Everywhere on the Telescope

Thermocouple sensors plus multiplexors and A-to-D convertor VME modules with 0.1°C resolution are standard off-the-shelf components. I recommend that we procure a VME module for the alidade and one for the elevation structure, each with 256 channels, *if* the cost is reasonable.⁴ I suggest installing ≈ 200 sensors initially:

- Temperature sensors along each alidade leg, perhaps about 20 total, in order to measure thermal contribution to changes of elevation axle orientation. In principle we could install a sensor on each structural member of the alidade if necessary in order to fully model its thermal contribution to pointing.
- Temperature sensors attached to the backup structure all over the dish, perhaps about 50 total, in order to measure thermal changes of the size of the dish.
- Temperature sensors from the front to the back of the backup structure at several points across the dish in order to check on the temperature gradients from the front to the back of the dish, perhaps about 50 total sensors. This data will be introduced into the structural model in order to calculate the bending of the dish.
- Temperature sensors attached to the dish panels at several points to measure the difference between panel temperature and air temperature, perhaps about 10 total.

³An inclinometer operated by Brockway detected the June 28th earthquakes in California.

⁴The “RTD” system which has already been procured is more precise ($< 0.1^\circ\text{C}$) than we need for most of the temperature sensors and it would be expensive in a large installation ($\approx \text{US}\$175/\text{sensor}$).

Such differences (caused by solar heating and radiation cooling) may drive convection which will corrupt laser ranging measurements.

- Temperature sensors along the feed arm and around the subreflector and feed room, perhaps about 40 total, in order to measure changes of the size of the feed arm.
- Air temperature sensors along the alidade legs and the feed arm with ≈ 10 m spacing, about 40 total, in order to measure the variation of temperature with height and position for the laser rangefinders. If the thermocouples on the alidade legs respond quickly enough they should be able to measure correlated changes dependent on wind velocity and direction. See page 8 for a discussion of a more elaborate air temperature sensing system.

Potential of $10\mu\text{m}$ Cameras

An imaging camera operating in the $10\mu\text{m}$ wavelength range could see and measure the details of the temperature distribution throughout the GBT structure. Such data could be used to interpolate between and extrapolate beyond thermocouple data. We may be able to detect daytime convection due to solar heating around the dish and/or nighttime radiative and conductive cooling effects. Probably we would be able to get significant insight into the origins of a variety of thermal effects. Such a camera has been used around sub-mm telescopes and VLA and VLBA antennas [Jan91] and is being borrowed for tests at the 12-Meter. The fascinating discussions in [Jan91] of temperature differentials observed around VLBA and VLA antennas with an Inframetrics Model 525 IR Camera demonstrate conclusively that this technique can provide new insights into thermal causes of pointing error. I recommend that the GBT procure at least one of these instruments. We could capture a digital image of the temperature distribution with a frame grabber.

1.2.5 Refraction Models & Sensors

Chapter 13 of [TMS86] contains an excellent discussion of refraction, and the following paragraph is adapted from it. The refraction is given by Snell's Law, which is

$$n_0 \sin z_0 = \sin z, \quad (1.1)$$

where z is the zenith angle at the top of the atmosphere (where $n = 1$), and z_0 is the zenith angle at the surface (where $n = n_0$); this equation is true for a plane-parallel atmosphere regardless of the vertical distribution of the index of refraction. For an atmosphere consisting of spherical layers, the angle of refraction, $\Delta z = z - z_0$, is given [Sma62] by the formula

$$\Delta z = r_0 n_0 \sin z_0 \int_1^{n_0} \frac{dn}{n \sqrt{r^2 n^2 - r_0^2 n_0^2 \sin^2 z_0}}, \quad (1.2)$$

where r is the distance from the center of the earth to the layer where the index of refraction is n and r_0 is the radius of the earth. For small zenith angles, expansion of (1.2) gives

$$\Delta z = (n_0 - 1) \tan z_0 - a_2 \tan z_0 \sec^2 z_0 \quad (1.3)$$

where a_2 is a constant. The “refractivity” N , defined by $N = 10^6(n - 1)$, of moist air in the radio range is given by the empirical Smith-Weintraub formula

$$N = 77.6 \frac{p_D}{T} + 64.8 \frac{p_V}{T} + 3.776 \times 10^5 \frac{p_V}{T^2} \quad (1.4)$$

where T is the temperature in Kelvins, p_D is the partial pressure of dry air, and p_V is the partial pressure of water vapor in millibars (1 mb=100 newtons/m² =100 pascals; 1 atmosphere=1013 mb). Eq.1.4 is accurate to better than 1% for frequencies below 100 GHz; the accuracy can be improved by adding a small term that increases monotonically with frequency by about 0.5% at 100 GHz and 2% at 200 GHz. The refractivity can be expressed in terms of gas density, using the ideal gas law,

$$p = \frac{\rho R T}{\mathcal{M}}, \quad (1.5)$$

where ρ and p are the partial pressure and density of any constituent gas, R is the universal gas constant (8.314 J/mol/K) and \mathcal{M} is the molecular weight, which for dry air in the troposphere is $\mathcal{M}_D = 28.96$ g/mol and for water vapor is $\mathcal{M}_V = 18.02$ g/mol. The total pressure and density are the sums of the partial pressures and densities, so substitution of Eq.1.5 and $\rho_D = \rho_T - \rho_V$ into Eq.1.4 yields

$$N = 0.2228 \rho_T + \left(0.076 + \frac{1742}{T}\right) \rho_V \quad (1.6)$$

where ρ_T and ρ_V are in g/m⁻³. Eq.1.6 defines the “dry” and “wet” refractivities. The dry part of the refraction is well behaved; the wet part is a problem in the radio range because it is strong and variable.

Weather Station

Refraction depends on several environmental variables, for which we must have sensors:

air temperature to 0.1 °C

air pressure

humidity

22 GHz Sensors for Wet Refraction

[TMS86, p.436, “Water Vapor Radiometry”] discuss how the excess propagation path (or, equivalently, the index of refraction) in a particular direction due to water vapor can be determined from measurements of the brightness temperature in the same direction at frequencies near the 22.2 GHz water vapor resonance. The sensitivity of T_B to pressure is decreased by moving off the resonance frequency to a frequency near the half-power point of the transition. At 20.6 GHz the absorption is nearly invariant with pressure.

The brightness temperature at 22.2 GHz has been found empirically to be related to the wet path length by the equation

$$T_B = 2.1\mathcal{L}_V, \quad (1.7)$$

where \mathcal{L}_V is in cm.⁵

The water droplet content in clouds causes substantial absorption but small change in the index of refraction compared to that of water vapor. In order to eliminate the brightness temperature contribution of clouds, measurements must be made at two frequencies, ν_1 and ν_2 , one near the water line and one well off the water line, respectively. The brightness temperature is

$$T_{Bi} = T_{BV_i} + T_{BC_i}, \quad (1.8)$$

where T_{BV_i} and T_{BC_i} are the brightness temperatures due to water vapor and clouds at frequency i . The temperature of the clouds is $T_{BC} \propto \nu^2$, so the observable

$$T_{B1} - T_{B2} \frac{\nu_1^2}{\nu_2^2} \quad (1.9)$$

will eliminate the effect of clouds.

The measured T_{H_2O} implies the integrated density of water along the beam.⁶

Dave Hogg put in a request for the last of the 225 GHz (H_2O band) radiometers which were built for the mmA site surveys;⁷ I hope that GBT gets it to use for a comparison during the winter.

Anomalous Refraction

Rapid variability of the wet refraction is referred to as “anomalous refraction”; it is due to moving bodies of water vapor causing “wedges” which refract the beam. A recent paper by Coulman [Cou91] concludes: “On the basis of measurements of atmospheric humidity fluctuations... it is possible to calculate likely maximum values for anomalous refraction effects on radio observations at millimeter and centimeter wavelengths. The following tropospheric phenomena have been shown to produce effects which agree in order of magnitude with the observations of apparent displacement of known radio sources:

1. dispersal of nocturnal inversions,
2. mixing through the capping inversion of the planetary boundary layer (PBL),
3. mixing through the sub-cloud layer,
4. convective structure in the PBL and
5. the passage of cold fronts.”

⁵finish this discussion using relationships derived on pp.410-411 of [TMS86].

⁶need figure of 3 sensors around beam

⁷described in a memo in the mmA series.

The humidity variations also cause phase variations, which have been studied for many years in the context of interferometers. [TMS86, p.428] contains a discussion of atmospheric phase fluctuations due to variations of the water vapor distribution; table 13.2 on p.436 gives measured values of the turbulence parameter $C_n^2 L$ observed with various interferometers. The resolution of a map produced by an interferometer is degraded since the derived map is convolved with a Gaussian beam of width θ_s , the seeing angle, which is given by

$$\theta_s = 1.08 \times 10^6 (C_n^2 L)^{3/5} \lambda^{-1/2} \quad (1.10)$$

in arcseconds. The entry for the Green Bank interferometer says $C_n^2 L = 5 \times 10^{-13}$ to $5 \times 10^{-11} \text{ m}^{1/3}$ for $\lambda = 11 \text{ cm}$; the latter value yields **0.9 arcsec** as the “seeing” width. On p.436 [TMS86] say: “The strength of the phase fluctuations, characterized by the parameter $C_n^2 L$, is difficult to predict. Measurements at the VLA show that $C_n^2 L$ is not well correlated with surface absolute humidity. The dominant correlation is probably with solar-induced convection... [phase variations appear to have] strong positive correlation with temperature and duration of sunshine, and negative correlation with cloud cover.” While it is appropriate to be pessimistic about precision pointing on a sunny summer day, this pessimism about anomalous refraction should be balanced with the following assertion from [Hog89, p. 2]: “I think that it is very likely that there will be no anomalous refraction effects during observations on winter nights in Green Bank.”

MPIFR reports of tens of arcseconds. Hogg [Hog89] references various papers. The MMA will have essentially the same problem with anomalous refraction. [Lam92a]

Methanol Maser Sensors for Wet Refraction?

Mike Balister has suggested installing several 6 GHz feeds around the main GBT feed to act as an interferometer which could measure the pointing of the beam relative to any methanol masers within a field of view of perhaps 40 arcmin. There are 50-75 of these masers, mostly along the Galactic plane, so the scheme would apply to less than 100 deg² out of the 40,000 deg² of the sphere. An important class of high-frequency target will be extragalactic CO, and the methanol masers will not help at all for this. I conclude that this concept is not as attractive as other ideas discussed here, but it should be remembered if Galactic plane work in regions near methanol masers becomes popular.

Multi-Beam-Mapping—Self-Cal for Single-Dish?

Pointing problems do not always need to be solved in real-time. Interferometers cope with phase (pointing) variations by utilizing the “self-calibration” technique during data reduction; redundant measurements allow solving for time-variable phase corrections on a per-antenna basis. A similar technique is probably feasible for single-dish telescopes like the GBT if maps are constructed by scanning multiple beams rapidly. As with interferometers, the technique would only work if there is at least one “sharp” source in the field of view that is detectable in an integration time comparable to the timescale of typical phase variations. The idea is to solve for a time-variable offset of the field center while simultaneously solving for the mean map produced from many scans over the target region.

Point sources or edges in the target will appear at the wrong time or in the wrong beam whenever refraction has shifted the field. This approach to single-dish mapping would require substantial CPU power and data storage capacity in order to produce maps by what would be, effectively, a combination of self-calibration plus “basket-weaving”.

An interesting experiment would be to scan a strong source with the 140-Foot and the 6 Ghz 7-beam feed while simultaneously observing with a 22 GHz radiometer. Apparent movement of the source could be seen in the 7-beam data and could be correlated with fluctuations in the water vapor.

Optical Telescope Sensor for Dry Refraction

A sensor attached to the telescope which views the sky in the optical band is essentially unaffected by the refraction due to water vapor. It can, therefore, be used to verify that the “dry” part of the refraction correction (proportional to the total number of O_2 molecules along beam, i.e. ratio of pressure to temperature) is operating correctly.

A commercial 30 cm Schmidt-Cassegrain with a commercial ($\approx 500^2$) CCD camera could be mounted on the feed arm parallel to the radio beam to see stars at night. The field of view might be ≈ 5 arcmin with ≈ 0.5 arcsec resolution. The telescope would be mounted on a small-angle (few minute of arc) drive so that it could integrate in spite of vibrational and scanning motions of the GBT. The optical telescope would enable us to measure and eliminate pointing errors due to changes in the dry refraction during night-time operations. The goal of specifying a comparatively large aperture and a sensitive detector is to enable the telescope to detect most of the 18×10^6 sources in the HST Guide Star Catalog, i.e. to be able to detect an optical pointing calibrator source in almost any small field of view *while the GBT is observing*. If a smaller optical telescope and/or poorer detector is specified the system would only acquire pointing information from bright sources during special pointing calibration observations. Such a lower performance system could still be a “good thing”—the 12-Meter has benefitted considerably during the past year from such a system.

I am concerned that the drive system for the telescope and/or the CCD camera system would emit RFI too near the feed room. I am also concerned that the development of software for such a complicated sensor could be a time-consuming investment with only marginal gain for the overall PPS of the GBT. I propose to defer implementation of this concept until 1994 at the earliest, and probably until 1995, but I recommend that it be retained as an optional item in budget plans.

Ionospheric Refraction

Ionospheric refraction can be ignored for the GBT. [TMS86, Table 13.3, p.440] says that the maximum likely daytime ionospheric refraction at 100 MHz for a zenith angle of 60° is 0.05° (180 arcsec) with a frequency dependence of ν^{-2} . This implies the worst-case at 1 GHz is ≈ 2 arcsec, far smaller than the ≈ 600 arcsec beam width of the GBT at 1 GHz.

1.2.6 Wind Sensors

Velocity Sensors

We need wind velocity sensors. Ideally such sensors should be mounted on 50 m towers in a ring around the GBT, so that there is always a sensor upstream from the telescope. This may be too expensive. It is unclear what the appropriate compromise will be.

Pressure Sensors

C. Merrill has suggested [Mer92a] that at least four differential pressure sensors be installed on the GBT dish. He states that the instantaneous lift and drag forces on the dish (a big airfoil) can be inferred from the pressure readings. These lift and drag forces can be introduced into the structural model to calculate distortions of the structure.

Torque Motor Current Sensors

The motor currents in the azimuth and elevation drive servos will be sensed by the M&C system, and will be provided to PPS. These currents indicate the instantaneous torque forces which the drives are applying to counteract torques on the telescope structure produced by wind. This data should also enable us to estimate the power spectrum of wind turbulence noise up to the bandwidth cutoff(s) of the servo(s). We will want to compare the measured torques to values computed by the structural model from the average wind velocity and from pressure sensor readings.

1.2.7 M&C Motion Plan

The M&C system will inform the PPS of the motion commands it intends to issue during the next few seconds. This will permit the PPS to calculate structural deformations which will be produced by the planned accelerations, and supply the resulting revised pointing offsets to M&C on the next information exchange cycle (10 Hz?⁸). We must take care that the time delay between plan and response will not cause an oscillating solution. Probably this can be assured by limiting the bandwidth of this loop to half the bandwidths of the individual systems.

The purpose of utilizing motion plans is to permit M&C to take data during more of the acceleration and deceleration phases of raster scanning, i.e. to increase the duty cycle during mapping operations.

The dish shape will be changed by acceleration loading. This will not only change the direction in which the centroid of the beam is pointing, it will also broaden the beam (departure from proper paraboloid). Such broadening will not be correctible with the active surface system, and therefore it may not be appropriate to integrate signals higher than some upper-limit frequency while the telescope is accelerating. This means that PPS should supply a predicted broadening to M&C so that it can decide whether to integrate during acceleration.⁹

⁸TBD

⁹add to interface list!

M&C Algorithms

Certain algorithms should be used in the M&C system so that the GBT will have proper dynamical response:

Jerk Limiting Vibrations induced during motions are not caused by acceleration *per se*, but by *change of acceleration*, which is called “jerk”. Such vibrations can be limited by limiting the jerk. We need to derive analytic solutions for jerk-limiting acceleration profiles, along the lines of [Sch91]. If possible it would be nice to have a derivation of the power spectrum of jerk-limited motion.

Bandpass Splitting We will send low frequencies of motions to the Az-El drives and the high frequencies to the subreflector actuators.

Servo Response Prediction The beam must follow the correct trajectory—the combined effect of the trajectories of Az-El and subreflector must produce the desired trajectory of the beam on the sky. This requires that M&C command motions which the servo and telescope can actually execute in a consistent fashion. This does not mean that the servos must avoid non-linear regimes; rather, it means that if we saturate error signals we must do so on the basis of quantitative prediction, and must command other servos in a manner consistent with the saturation.

1.2.8 Radio-Source Observations

Observers will perform traditional pointing checks. The M&C system should include the ability to utilize offsets derived from such observations of calibrators. A major objective of this strategic plan is that the PPS of the GBT will be so effective and so reliable that most observers will trust it, and will make fewer pointing check observations. During the early testing phase we will want to observe numerous calibrators and utilize Condon’s FFT-fitting approach to verify that the PPS removes all systematic trends from the pointing errors. All pointing calibration observations will be logged for offline analysis, and will be retained for long periods of time.

1.3 Analysis Techniques

The concept is to adjust the coefficients of a complicated model until they fit the measured data of several kinds. The model will include temperature and wind data. It will be a finite-element structural model. The model parameters will be determined with a differential correction which will take O-C ranges (and autocollimator O-Cs) on its RHS. An F-test will activate and deactivate terms in the model. Different parts of the model may vary at different rates and will be solved independently at different rates with the various solutions being combined consistently. The end-result of the model is an algorithm which can compute the position and orientation of any element of the GBT relative to piers in the ground around the telescope. “Any element” includes the optics, so this strategic plan implies the ability to compute both the direction and the shape of the radio beam as a function of time.

1.3.1 Structural Modelling

The displacement of the structure is related to forces applied by

$$K\vec{u} = \vec{p}, \quad (1.11)$$

where K is the stiffness matrix, \vec{u} is the displacement vector and \vec{p} is the load (force) vector. Each element of \vec{u} (and \vec{p}) is *six* numbers, three of them coordinates (forces) and three of them rotations (torques). This is a system of simultaneous linear equations; the right-hand-side (force) is known and we solve for \vec{u} .

Differential thermal distortions can be modelled by a simple trick: the stresses in various elements caused by temperature changes are calculated with the ends constrained and the resulting (virtual) force vectors are added to nodes of \vec{p} at the ends of the elements. Gravity distortions are modelled by adding vectors to \vec{p} proportional to the mass at each node. Acceleration distortions can be modelled by adding torques to the proper nodes of \vec{p} . Distortions induced by wind lift and drag forces can be modelled by adding force (differential pressure) vectors to \vec{p} ; [Mer91] discusses examples of such calculations. Propagation of the effects of the alidade track irregularities can be modelled by adding displacements to the nodes of \vec{u} which represent the alidade trucks; these nodes are boundary conditions of the structural equations and are zeroed in an ideal model. Twisting of the alidade resulting from the irregularities (see [Con92] for a discussion of the twisting), as well as from acceleration, wind and differential thermal effects, will appear as the rotation components of the elements of \vec{u} , and these rotations can be compared with autocollimator and inclinometer measurements, while the coordinate components of \vec{u} are being compared with laser rangefinder measurements. The twisting forces due to wind appear as forces on the alidade trucks in the model, and after (1.11) is solved we can back-substitute the displacement solution \vec{u} into the equations for the constrained nodes at the base to solve for the reaction forces, which can then be compared with the azimuth torque motor currents (obviously an analogous calculation can be compared with the elevation currents).

The coordinate components of \vec{u} for the dish portion of the elevation model will be used to implement the open-loop surface control. The coordinate components of \vec{u} for the feed arm portion of the elevation model will be used to implement the open-loop control of the position and orientation of the subreflector to compensate distortions of the feed arm. The conclusion of [Sri92] (which is based directly on the NASTRAN models) is that: “the subreflector translations can largely compensate for the loss of efficiency caused by gravity-induced deformations, provided the active surface has been used to remove the surface rms errors. The [gravity-induced] pointing errors addressed in this memo are assumed repeatable and, if repeatable, can be corrected through the antenna az-el drives.”

NASTRAN Timing Estimates

NRAO uses the NASTRAN package from MacNeill-Schwindler for structural analysis. The production PPS will probably use a mathematical library (perhaps a C++ class) to solve structural problems, which will probably be faster than NASTRAN for our particular problem. For the purposes of this memo NASTRAN timings are a conservative estimate.

Section 3.4 of [MSC91] gives the timing formula for solving the static structural equation problem

$$T = \frac{1}{2}NMC^2, \quad (1.12)$$

where T is CPU time in seconds, M is the machine speed constant in seconds, N is the number of degrees of freedom of the model and C is the RMS number of “active columns” (the number of non-zero coefficients per row of the sparse matrix). NASTRAN’s current coefficient M for a Sun SPARCstation-2 is 0.754×10^{-6} s. The combined alidade plus elevation model of the GBT, complete except for mid-beam actuators, has $N = 10744$ and $C = 654$, and (1.12) predicts 1732 s.¹⁰ The number of non-zero coefficients in the sparse matrix should be about NC , $\approx 7 \times 10^6$ in the GBT case.¹¹

Price-performance is doubling every year and CPUs are becoming concurrent. It is reasonable to suppose that by 1994 we can procure a multi-CPU system with

$$M_{94} \approx \frac{M_{91}}{4 \times 2^{(94-91)}} \approx \frac{M_{91}}{32}, \quad (1.13)$$

where M_{91} is the NASTRAN value for the SPARCstation-2, a 1991-vintage single-headed CPU. If so, then **we could compute the full GBT model in ≈ 54 s**, fast enough to track changes of gravity, temperature and average wind loading. This is the key strategic concept of the PPS plan.

We will be able to compute structural models somewhat faster than the above estimate, for the following reasons:

- The number of degrees of freedom used in the current GBT models is larger than it needs to be for purposes of estimating pointing corrections. Elements can be grouped into lumped masses (normal points) and adequate prediction accuracy can be verified with numerical tests. Chris Merrill speculates that N as small as ≈ 3000 might be good enough for pointing calculations.
- The alidade, elevation and feed arm groups of equations can be solved as separate problems, with different update frequencies corresponding to different rates of change of independent variables.
- Each new solution is only ϵ away from the previous solution and there are solution techniques which run faster in such cases.
- Probably some tuning of the sequencing generator for the structural equations will decrease C , perhaps to as low as ≈ 400 (note that timing is proportional to C^2).

The combined effect of these improvements will probably enable us to compute a GBT structural model in 10-20 s in 1995.

¹⁰Our SPARCstation-1 (gbtsp3) gets 3620 s, reasonably consistent with expected speed ratios.

¹¹Our NASTRAN disk file is ≈ 32 MB, $\approx 20\%$ larger than 4 bytes/coefficient.

1.3.2 The “Rubber-Sheet” Function

The details of the structural model (e.g., as-built dimensions of members) must be adjusted to conform to measurement data, because the structural model will not be correct to one part in a million initially, and because there will surely be un-modelled physical effects that will produce small differences even after the initial adjustment of the model. *I assume that these differences can be modelled with sufficient accuracy by as a smooth function, some type of low-order polynomial. This is a critical assumption of this strategic plan.*

The adjustment will be made by scaling the displaced coordinates computed by the structural model, using a formula something like

$$\vec{u}'_j = (\vec{u}_j + \vec{u}_{j,0}) \left(1 + \sum_{k=0}^n \alpha_k P_k(\vec{u}_j) \right), \quad (1.14)$$

where \vec{u}_j is the computed displacement of the j -th node, $\vec{u}_{j,0}$ is the location of that node, and α_k are the coefficients of a suitable polynomial $P_k()$ as a function of the coordinate system of \vec{u}_0 . Note that the polynomial multiplies the coordinates, rather than adding, so that it can keep the coordinate origin invariant. It is added to one so that we will have $\alpha_k \approx 0$ rather than $\alpha_k \approx 1$.

The order of the polynomial needed will depend on how well the structural models match the measurement data. The order will be adjusted automatically in the regression using a significance test.¹² This adaptive solution procedure will implement a rubbery mapping of the structural model onto the real structure as revealed by the laser and autocollimator data. It will absorb unknown or as-yet-unmodelled physics. Our long-term goal will be to reduce the magnitude of this function to zero in the limit as our knowledge improves.

1.3.3 Bootstrapping Retroreflector Coordinates

Initially no coordinates are known. Even after the coordinates have been calibrated we will want to introduce new retroreflectors, and we will need to calibrate their coordinates. In general, the coordinates don't change (if the coordinate system is properly defined), so it will be appropriate to lock them once they have been adequately determined, and then use them to infer changes in the structure. I call this process “bootstrapping”. The philosophy is that the incoming datastream has a certain statistical weight, and we wish to apply that weight optimally to estimate corrections to several thousand unknowns, and we will therefore use an adaptive solution which turns variables off in the regressions whenever they become known well-enough.

Another philosophical attitude embodied in this plan is that while we pretend that we are making absolute determinations (and it will be a rather good pretense), the plan can equally well be viewed as simple change monitoring of the style which has been discussed frequently in GBT memos about active surface control. The absolute coordinates will be numbers with more than 20 bits of significance, but many of the key servoing actions of

¹²The F-test(s) will be implemented using the algorithms referenced in the description of the stepwise regression subroutine RSTEP in the IMSL library. [IMS87, p.183-192]

the PPS will mostly depend on *differences* of those numbers, and we can be much more confident about the truth of those differences than we can be about the high precision absolute values. The important thing is *local consistency* in the coordinate system, so that calibrations can be interpolated and extrapolated reliably.

Az/El Geometry Determination

The laser rangefinders on the piers will range on each other; their coordinates relative to each other will be determined. We will define an arbitrary origin and orientation, probably something like the centroid of the ring of rangefinders on piers (i.e. approximately the pintle bearing) and the mean plane fitted through them. At first the orientation of this plane relative to the sky will not be known; it can be calibrated either by observations of optical calibrator sources using TV cameras in one or more rangefinders or by observations of radio calibrator sources using the GBT itself.

A retroreflector on the alidade is attached to the rotating coordinate system of the alidade. Its location in that system can be determined by ranging on it from the piers while rotating the telescope in azimuth.

Likewise, a retroreflector on the elevation structure is attached to the rotating coordinate system of the elevation structure, which is attached to the rotating coordinate system of the alidade. Its location in the elevation system can be determined by ranging on it from the piers while moving the telescope in both azimuth and elevation.

Dish/Feed-Arm Geometry Determination

Retroreflectors in the upper part of the elevation structure which are not visible from the piers will be calibrated by measurements made by rangefinders on the feed arm. The coordinate system of those measurements will be calibrated by measurements on the retrospheres, which will be calibrated from the piers. In certain elevations some such retroreflectors may become visible to the rangefinders on the piers, and such data may also be used.

Benchmarks

It will be useful to install certain retroreflectors and retrospheres with precisely measured offsets from certain key structural members or nodes, so that these retroreflectors can be regarded as “benchmarks” in order to facilitate bootstrapping of nearby retroreflector coordinates by interpolation. In particular, it would be very nice if a few such benchmark reflectors could be attached to certain actuators in some fashion such that they would point down instead of up and have known vector offsets from the surface retroreflectors attached to those actuators. This would tie the coordinate system of the front of the dish to that of the backup structure directly, effectively superceding the indirect path through the retrospheres, and strengthening the rôle of the pier rangefinders in the control of the surface.

Rôle of the Rubber-Sheet Function

The retroreflector coordinates determined by these calibrations will be vector displacements from a nearby node in the structural model. As the node is displaced and rotated the computed vector displacement will likewise be displaced and rotated to follow the motion of the bracket which holds the retroreflector. As the calibration process proceeds, adding more and more retroreflectors to the calibrated set, the rubber-sheet function will be produced as well. Canonical coordinates of new retroreflectors can be more rapidly inferred using the corrections supplied by the rubber-sheet function. It will act as an *interpolator* of inferred corrections to the computed geometry.

Noise Problems When Bootstrapping

Atmospheric refraction-index perturbations, differential temperature distortions and instantaneous wind loading effects can corrupt the process of bootstrapping, even though automatic corrections will be applied for these effects. The software will be designed to be robust in this sort of environment, but it will surely work best in benign conditions. Range residual data will be evaluated during normal operations, and if systematic trends on individual retroreflectors are detected during benign conditions, the coordinates will be updated.

1.3.4 Offline Analysis

We will log both measurement data and model solutions as function of time. We will retrieve the data later, as a background process while operating (implies we need some reserve power margin in CPUs) and use it to improve models. In particular, we want to analyze various trends in the model solutions (rubber-sheet functions) to detect missing or incorrect physical effects in the models, with the aim of driving the rubber-sheet functions to zero.

The rangefinder data acquisition rate is ≈ 100 ranges/s. This is 10^7 ranges/day, or 3×10^8 ranges/month. If we have 16 bytes/range, the rate will be 4 GB/month. Perhaps the appropriate response to this is to condense the data in some fashion, maybe by saving the rubber-sheet function plus range data that differs from it by a statistically significant amount. Alternatively, we could decide to buy enough disks to save several months of the latest data, plus “interesting” data (both very good and very bad conditions). Disks are getting cheaper; we can probably afford to save three months worth of data.

The organization of the database of raw data and model parameters (which are intimately related to the model functions) is one of the messiest technical problems of the whole project, and is probably the software problem which is least well understood at this time. The problem is that we want to change models in a flexible fashion while preserving proper interpretation of old data. It is likely than an Object-Oriented-Database [OODB] will be an effective approach to this problem. The choice of appropriate database technology will be made during the first year of the project.

1.3.5 Vibration Modes and Pointing

Wind turbulence noise will cause the GBT to vibrate. It is unclear what will be the coupling efficiency between the wind noise and the structure. It will be prudent to assume that the problem will be important at least some of the time. Probably we should implement at least some portion of the plan discussed in this section.

Modes and Models

The lowest—and probably most important—modes will be the lateral fork displacement of the alidade at ≈ 0.57 Hz [Kin92a, Mer92b, vH90] and the vertical torsional vibration of the fork at ≈ 0.7 Hz. The latter displaces the radio beam in azimuth. The feed arm will vibrate in azimuth at ≈ 0.7 Hz and in elevation at ≈ 0.9 Hz, and both of these are probably pairs of closely spaced frequencies due to the slight asymmetry of the arm. C.Merrill [Mer92b] expects a *minimum* of ten modes below 2 Hz.

Each mode is a damped harmonic oscillator with a nominal $Q \approx 50$. Such a high Q at such a low frequency implies that a vibration will have significant amplitude for tens of seconds once it is excited. The damping of the structure will probably be somewhat higher (lower Q) under wind loading [Kin92a].

The effect of each mode on the structure is described by its associated eigenvector, which can be computed by the dynamical analysis of the structural model. The vibrational state of the structure as a whole will be a linear superposition of the modes. Thus, the position of a node on the structure can be calculated as the static solution at that node plus a weighted sum of several eigenvectors, with the weights being the instantaneous damped amplitudes of the sinusoids of the modes.

Tracking the Modes

Each mode can be described by an amplitude and phase, or equivalently a single complex number. The complex number will be a function of time, and will execute a random walk due to impulses from wind noise. We can fit a low-pass continuous complex function for each mode to the ranging data and can use the function to *predict* the future motion of the beam. We can drive the subreflector.¹³ This is a “feed-forward” technique, an example of a Kalman filter.

Some (all?) mode frequencies will be functions of the elevation of the telescope, because of the change of moment of inertia with elevation. Also, the damping coefficients of the modes will be variable [Kin92a] in addition to being different from each other and unknown a priori. We will implement solutions for frequencies and damping coefficients with outer low-bandwidth software servo loops.

Driving the Subreflector

Brockway has discussed [Bro90b] the use of two-axis tilting of the subreflector with fast response to compensate pointing errors; he also cites three prior memos on the subject.

¹³need to discuss interaction issue

For GBT vibrations, the basic idea is to drive the subreflector with motions predicted by the modal tracking solutions so as to keep the beam stationary.

Wind noise is almost always present, so there will almost always be some energy in the modes, and this means that the subreflector will almost always be in motion with some amplitude at frequencies above 0.5 Hz. It also implies that the higher the frequencies allowed by the subreflector actuator servos the more modes we can track. Because the power in the modes decreases almost monotonically with mode number (frequency), the necessary subreflector drive amplitude decreases with frequency. This is a very reasonable situation from the point of view of the servo system, and it would be reasonable for the servo bandwidth to be increased from the present 1 Hz specification up to, say 2-3 Hz, but with decreased amplitude.¹⁴

Driving the subreflector in this fashion will only be practical if it does not excite significant deflections or oscillations elsewhere in the structure. At the present time a quantitative estimate of the coupling has not been made.

1.3.6 Adaptive Measurement Techniques

The proposed approach, which evolves an open-loop model using O-C residuals from measurements, can use whatever data are available. As data inputs are deleted the errors of the model will increase progressively, to provide a graceful degradation to the state of a static open-loop model — “static” only in the sense that no new range/angle measurement data can check the model, but not really static because gravity, temperature and wind changes will still be computed.

How often should a given retroreflector be measured? If rangefinder resources are limited we will want to measure the retroreflectors which will have the maximum impact on the variance of the model solutions. The development of an appropriate response to this concept will be an interesting and challenging part of the project.

One sophisticated approach would be to work backwards from the pointing error on the sky to infer the errors of the rubber-sheet function, and then to project those errors back to individual range measurements. We can compute how much the variance of fit of the beam position would decrease if we added one more measurement of a particular range. We can do this for all possible ranges, and then rank them in order of significance, so that we can make measurements in the order of this list in order to decrease the variance most rapidly.

Initially we will implement a simple heuristic round-robin scan, with different rates for different groups of retroreflectors, and perhaps with some dynamically adjusted adaptation of the relative rates between groups. Analysis might show that this design is good enough for the final system.

¹⁴need statement of achievable amplitude of motion of the actuators as a function of frequency. this is derivable from acceleration limit.

1.3.7 Potential of Neural Nets

Some systems analogous to this one have recently been using “neural-net” techniques to implement self-training adaptive Kalman filters. During the course of this project we will investigate the state-of-the-art in these technologies to determine whether it has application to the GBT. Two areas which look promising are enhanced mode tracking using data from upstream wind sensors and enhanced anomalous refraction tracking using upstream 22 GHz water vapor sensors. Any implementation of these ideas will be deferred to 1995+.

1.4 Surface Control

If we know where the backup structure is located, and we know where the surface is relative to the backup, and we know where the front-side retro-reflectors are located relative to the surface, we can calculate the shape of the surface. We can decide what shape we want, and can then download the difference as commanded motions.

It is unclear to me what surface we should strive to maintain; the two obvious possibilities are (1) best-fitting-parabola [BFP] and (2) fixed nominal shape. This question was debated by D’Addario and Thompson in two early GBT memos [D’A89, Tho89]; the arguments pro and con given by them are still relevant. I myself am unsure which mode to choose. We can build the PPS software to support either, or both, of these modes. We can also implement an additional shaped-surface correction if the case is made that it would be a “good thing”.

1.4.1 Open-Loop, Closed-Loop

The basic control of surface shape will be open-loop. I.e., once the system is calibrated it will be able to operate without new laser rangefinder data. This will make the system robust against rangefinder failures and will increase the bandwidth of the surface servo while reducing the required rangefinder measurement rate.

The formulæ are messy, and I am not confident that my reasoning about them is correct yet. The calculations will be done in the elevation structure coordinate system used by the structural model. The primary calculation will be something like

$$\vec{\delta}_i = (\vec{t}_{\rho,\theta} - (\vec{u}'_j + \vec{a}_i)) + \vec{c}_{\rho,\theta}, \quad (1.15)$$

where $\vec{\delta}_i$ is the computed position in the i -th actuator, $\vec{t}_{\rho,\theta}$ is the desired analytic form for the surface (see Sec. 1.4) probably expressed as a Zernike polynomial, (ρ, θ) are the surface coordinates of the i -th actuator, \vec{u}'_j is the displacement of a node close to the actuator which is extracted from \vec{u} (see Eq. 1.11) and is corrected with the rubber-sheet function (see (1.14) in Sec. 1.3.2), \vec{a}_i is that actuator’s zero point calibration (offset from \vec{u}_j to the actuator), and $\vec{c}_{\rho,\theta}$ is the closed-loop correction (probably zero, see below). The variables in (1.15) are vectors in order to emphasize the 3-D character of the problem, but in actual practice (1.15) will be approximated to produce scalar δ_i actuator corrections approximately normal to the surface.

Equation (1.15) will be a *closed-loop* surface servo whenever the rangefinders are operating, because the rubber-sheet function, which enters the calculation of \vec{u}'_j , will be continuously adjusted with the rangefinder data. This fact has the following implications:

- Measurements of retroreflectors on the backup structure will contribute to the surface servo by changing the rubber-sheet function.
- Measurements of actuator retroreflectors will contribute to surface control over a region size set by the maximum order of the rubber-sheet function (analogous to the wavelength of a spatial frequency cutoff). This means that it will not be necessary to measure *every* actuator retroreflector in normal operation. Indeed, because most of the needed surface corrections will be computed by the structural models, which will include effects of gravity, temperature, and wind, the surface servo will be maintained with a comparatively low rate of rangefinder measurements which are *sampling* the surface.
- Pointing and surface control will be intimately linked by the adaptive solution for the rubber-sheet function.

It is unclear whether $\vec{c}_{\rho,\theta}$ needs to be \vec{c}_i . My a priori assumption is that displacements of individual actuators will be highly correlated with displacements of adjacent actuators, so that $\vec{c}_{\rho,\theta}$ is the correct form. I further assume that $\vec{c}_{\rho,\theta} \approx 0$, i.e. that the rubber-sheet function which describes the (smooth) displacements of the backup structure will also describe the (smooth) displacements of the surface. This means that I expect that there may be no need to solve for $\vec{c}_{\rho,\theta}$.

1.4.2 Surface Servo

Commands to correct surface errors δ_i will be issued if $\delta_i > \frac{\lambda}{T}$, where tolerance T will be of order 16. This implies that the current highest observing frequency (shortest wavelength) must be supplied continuously to PPS by M&C. PPS will apply this test for each actuator at regular intervals and will issue individual motion commands to actuators. It may be appropriate to include a random element in the decision to issue a correction to an actuator in order to avoid producing structured patterns of surface residuals which would produce structured sidelobes [Sch90]; for example, we could do a “simulated annealing” type of calculation.

At the present time it is unclear whether the production version of the actuators will produce significant RFI for the GBT during low frequency integrations. Some observers might prefer that the surface servo operate while integrations are in progress so that they will have a correct surface at all times; others might prefer to have the same surface for one or more integrations. A flag will be available which M&C can set to inhibit the surface servo depending on the observing mode, observing frequency or observer’s preference.

1.4.3 The “Mouse”

The “mouse” will be a remote-controlled wheeled device carrying a retroreflector across the dish. The height of the retroreflector above the dish surface will be held fixed by

a simple servo. The three rangefinders on the feed arm will triangulate on the mouse relative to the nearby actuator retroreflectors. This will calibrate the positions of the panels relative to the actuator retroreflectors and will also map the shapes of the panels. Tables of computed adjustments for the panel settings can be computed from this data in order to position the panels to minimize overall setting error for each panel (best-fitting curve).

Suppose we wish to map the panels with 0.2 m resolution. With 6 laser rangefinders we can measure the eight retroreflectors in the corners of the two panels plus two independent mice at 5 Hz. The two mice would move 0.5 m/s, and together would map 0.2 m²/s. The 8000 m² of the GBT could be mapped in 40,000 seconds, about 12 hours. The result would be a 500² map of the 100 meter dish, more than 100 samples per panel, with an RMS of $\approx 100\mu\text{m}$, sufficient to resolve the large-scale manufacturing errors of the panels.

The mouse approach should permit us to set the surface with a precision comparable to the manufacturing accuracy of the panels, and to compute the direction of the beam produced by that surface relative to the orientation of the retroreflector spheres at the edges of the dish. The detailed maps of the surface should permit prediction of the width and sidelobes of the instantaneous beam.

1.4.4 Initial Adjustment of the Panels

During installation of the panels of the main dish a jig should be used to set the four corners at a chosen height above the retroreflector on each actuator. A spirit level on the jig or some sort of optical sight can be used to orient the jig so that the plane formed by the corners of four panels has the correct inclination and azimuth. This adjustment will permit the three lasers on the feed arm to correct the surface by driving the actuators, and the result should be good even before holography or a mouse-map can be performed.

The panels of the subreflector can be calibrated face-up on the ground using the mouse and three lasers temporarily mounted for triangulation. The panel can be set using distortions calculated for the situation when the subreflector is hanging from the feed arm face-down.

1.4.5 Holographic Measurements

If the mouse technique is successful it should enable the surface control portion of the PPS to set the surface with a precision comparable to the manufacturing accuracy of the individual panels. Such a success would mean that holography would no longer be critically needed for calibrating the surface. Instead, it would be used mainly as a check of the PPS surface control, a determination of the surface RMS as built. The quality of a holographic map is critically dependent on pointing as well as on the surface, so holography will be a critical end-to-end test of the entire PPS, the ultimate test to assure that no signs are backward, or trig terms complemented.

1.4.6 Beam Direction and Beam Shape

It is self-evident that complete knowledge of the geometry of the optics relative to the structural model nodes, which give instantaneous displacements and rotations, implies complete knowledge of the instantaneous beam direction and beam shape. I have not decided exactly how to carry out the computation, but I have spoken with Srikanth about his optics algorithms, and have inferred from the approximate timings that he quotes for his SPARCstation that the calculation will probably take only a few seconds with the CPU that we will procure.

1.5 Destinations for Pointing Information

Predicted Offsets to M&C Predicted pointing matrix transformation for all degrees of freedom of telescope, a function of focal plane coordinate system, is supplied to M&C as matrix with partials and derivatives to be valid for approximately the next 10 seconds, updated regularly (10 Hz?¹⁵).

Note that there is the potential for inter-process feedback loops that would oscillate because of the 100 msec interval between RPCs; this can be avoided by band-limiting the functions.

Corrections to Surface Servo Data rate is fairly low.

A Posteriori Offsets to Archive The offsets which will be sent to M&C in real time will be *predicted*, i.e. we will be applying a type of Kalman filter to the datastream of the rangefinders and autocollimator. The same datastream will re-analyzed a few seconds later, and improved estimates of instantaneous offsets will be produced. This problem is in the class of trajectory estimation, where knowing the mathematical form of a trajectory enables us to make a least-squares adjustment for the position at some instant using data from both before and after the instant. The final values of the pointing matrix transformation time series will be determined about five seconds after real time and will be sent to the archive so that data reductions can use these improved estimates.

¹⁵TBD

Chapter 2

Interfaces

describe software interfaces¹

2.1 Interface to M&C

The following items will be passed with a frequency of 10 Hz to PPS by M&C as the arguments of an RPC:

Focus Mode Prime focus versus Gregorian.

Frequency Current highest frequency, used for tolerance on surface servo.

Surface-Servo Disable Flag to disable the surface servo, generally to avoid RFI problems while integrating.

Trajectory Plan Anticipated trajectory for the next ten seconds for Az-El and the six subreflector actuators. PPS will use this (especially Az-El) to calculate pointing changes due to acceleration-induced twisting of the structure. The trajectory is a *function*, and will be expressed as either a Taylor series or a cubic spline.

The PPS will reply with the following result values:

Pointing Correction Plan Predicted difference between ideal Az-El coordinates and actual encoder coordinates as a function of focal plane coordinates, plus matrix of partial derivatives of ideal coordinates w.r.t. subreflector actuator coordinates.² The prediction will include focus relative to the instrument focal plane as well as position on the sky. The prediction is a *function*, and will be expressed as either a Taylor series or a cubic spline. *The exact mathematical form of this interface has not yet been specified; this will be a PPS task in 1993.*

The prediction will be given in terms of focal plane coordinates because there will be multiple feeds in the focal plane; M&C knows about them, PPS does not. On

¹need block diagram

²Note that this result will have a different form when in prime focus mode.

the other hand, PPS knows about refraction and the peculiarities of the subreflector actuator geometry, M&C does not. Focus will be computable from the prediction because M&C will need to be able to integrate with focal offsets for various reasons.

2.1.1 Asynchronous RT Processes

Telescope control systems built at NRAO and other observatories in the past have been *synchronous*: computations are performed, decisions are made and commands are sent to hardware at fixed regular intervals. The 300- and 140-foot telescopes ticked at 100 Hz, the 36-foot at 10 Hz, the VLA antennas at about 19 Hz, the VLBA at 20(?) Hz. The “hard” deadlines must be met for these systems to operate correctly. Precision computations of position can be made for the time of the next “tick” and can be loaded and armed to become effective at that instant. With proper techniques the necessary staging, allocation of CPU resources for computation and synchronization of actions can be achieved, and indeed *proofs* of the correctness of such synchronous designs can be produced.

For a variety of reasons it has been decided that the GBT will be—mostly—an *asynchronous* system. How can precision computations to be valid for particular instants of time be produced if there are no predictable particular instants? The answer is that we must calculate not a particular value for a particular time, but rather a particular *function* which will be valid over a period of time, and then the subsystem which receives the function can evaluate it for any instant which is needed. This approach removes the “hard” deadline constraints, but at the price that it is harder to produce a proof of correctness. It appears that this asynchronous approach will work, but we must acknowledge that there is little if any precedent for designs of this type at NRAO or other observatories.

2.2 Interface to Laser Ranging

We must define a protocol interface for communication between the PPS and the laser ranging instrument CPUs. This should be a remote procedure call (RPC) or equivalent. I recommend a function with 7 arguments:

$$laser(T, t, \xi, \eta, \dot{\xi}, \dot{\eta}, \dot{r})$$

T is the commanded integration time; it also acts as a flag which indicates whether the remaining 6 arguments are set. t is the time for which the remaining arguments are valid, ξ and η are the beam steering mirror angles, $\dot{\xi}$ and $\dot{\eta}$ are the angular rates and \dot{r} is the predicted range rate. If $T > 0$, the remaining arguments constitute a work order which the laser-ranger software will append to the queue of measurements to be done. It may be appropriate to limit valid values of T to be 2^n msec, with $n = 0, 1, 2, \dots$

The remote procedure call will return 9 scalar values

$$(S, N_i, N_o, \tau, \xi, \eta, \rho, \sigma, f)$$

where S contains the serial number of the laser-ranger instrument plus an instrument status code, N_i is the number of work orders outstanding in the input queue and N_o is the

number of results waiting in the output queue. τ is the time when the measurement was made (to millisecond accuracy). Whenever $\tau > 0$ the last 6 values are the results for one range measurement: ξ is the first mirror coordinate, η is the second mirror coordinate, ρ is the range result, σ is the r.m.s. of the ρ measurement and f is the measured flux. The calling program can make remote procedure calls with $T = 0$ (i.e., no command) to fetch results from the output queue until it gets $\tau = 0$ returned.

2.2.1 Implementation Details

- There should be a convention that the returned σ value will be set to some special value whenever the instrument software believes that no detection was achieved.
- Fluxes should be returned so that we will be able to “peak-up” on newly-installed retroreflectors, whose coordinates are not known precisely. The protocol will enable us to scan a raster centered on the moving (putative) coordinates of a new retroreflector and analyze the pattern of measured fluxes in order to locate the retroreflector.³ The flux values will be used by the Precision Pointing System to estimate attenuations due to fog and/or condensation.
- The laser-ranger instruments should execute successive work orders synchronously (successive integrations contiguous in time) so that a time series of commands for a target can be arbitrarily long when measuring vibration power spectra.
- When integration times are short procedure call rates will be high. Probably this will be acceptable if the RPCs are passed via a TCP virtual circuit rather than via single UDP packets, but if tests show that there is a problem the scalar arguments and values in the protocol can be changed to vectors.

2.2.2 Range-rate Requirement

An implementation detail of special importance (because it has not yet been demonstrated in the prototype system) is the requirement that the laser-ranging instruments accept predicted range rates as one of the arguments of their remote procedure call.

Consider the ring of laser-ranging instruments on piers $\approx 50\text{m}$ from the azimuth track. If multiple instruments simultaneously range on multiple retroreflectors on the four azimuth trucks the azimuth of the base of the alidade can be determined with high precision. If we wish to make such a determination while the telescope is scanning at maximum rate, the instruments will need to be able to derive ranges to moving targets. The maximum azimuth angular rate is 40 deg/min (0.0116 radian/s) and the radius of the track is 32 m, so the maximum range-rate will be 0.37 m/s. Range will change by up to $370\mu\text{m}$ per millisecond! The maximum range-rates for the elevation structure are similar (angular rate

³The prototype software has the ability to search for flux in an area of the angle space and print the location of a peak. I am recommending that this logic be moved to the PPS. The search operation will be performed only when a new retroreflector is introduced into the PPS database, so the bursts of data transmission on the LAN when searching will be infrequent. The search operation is not time-critical.

only 20 deg/min but radius more than 50 m). Range-rates are smaller at sidereal tracking rates, but still several times larger than RMS measuring errors for typical integration times. For example, a retroreflector at the radius of the dish, 50 m, moves 3750 $\mu\text{m/s}$ at sidereal rate, 480 μm during the standard integration time of 128 msec.

2.3 Interface to Active Surface

The active surface subsystem will move the actuators to requested positions. It will apply LVDT temperature corrections as needed. The zero point offsets of the LVDTs will be arbitrary and will be unknown to the active surface subsystem.⁴

The active surface subsystem will be able to move all 2213 actuators simultaneously.

We must define a protocol interface for communication between the PPS and the main CPU of the active surface subsystem. This should be a remote procedure call (RPC) or equivalent. I (tentatively) recommend⁵ a function with 3 arguments

$$\text{actuators}(n, a[64], x[64]), \quad (2.1)$$

where n is the number of values in the two remaining vector arguments, $a[]$ is a vector of actuator IDs and $x[]$ is a vector of desired actuator coordinates. We need a convention to indicate that an $x[]$ value is not valid, e.g. if $x[i] = -999$.

The remote procedure call will return three vector values

$$(x[64], t[64], s[64]) \quad (2.2)$$

where $x[]$ contains the LVDT coordinates which the active surface system sampled at times $t[]$ for the actuators specified by $a[]$ in the call, and $s[]$ is a vector of status codes for those actuators. The codes will have bits for the states “braked”, “reset”, “forward”, “backward” and “down”.

2.4 Interface to Autocollimator

Chuck Brockway has informed me⁶ that the autocollimator will deliver 6 channels of analog signal. Inclometers will need 2 channels, so we will have a total of 10 analog channels if two inclinometers are installed on the alidade. These signals are available on the alidade structure, near the electronics rooms. A VME-module A-to-D converter should be installed somewhere in that area to acquire these 10 signals. Probably a task in one of the M&C computers can log the data and pass it to PPS; if that is not convenient we can acquire an independent VME crate and CPU to do the job. The data rates are low, about 200 bytes/s of data.

⁴We must worry a little bit about temperature effects within the actuator/LVDT assemblies which might not be properly accounted for by simple offset vectors from structural model nodes. Probably this is not significant, but it needs to be checked.

⁵based on conversation with T. Weadon 30-July, cite this.

⁶cite this

2.5 Interface(s) to Environmental Sensors

Thermal sensor system⁷, 10 μ m camera, optical telescope, wind sensors⁸, air microthermal sensors⁹.

2.6 Interface to Operator & User

Certain flags and values to be supplied by M&C, particularly observing frequency (which will control the surface servo “tightness”) and a surface servo on/off flag. M&C will control whether subreflector or tertiary move the beam, so user can enable these by talking to M&C alone.

Other commands will enter the PPS via a graphical user interface [GUI], probably under PV-WAVE. This will be, of course, implemented as an X-windows client process, which permits display on any X-server anywhere on the Internet.¹⁰ Probably the command set will include options to activate/deactivate various data sources and command outputs. For example, we might want to deactivate the autocollimator, or the optical telescope, or one of the laser rangars, or the surface servo, or feed arm tracking with the subreflector.

The most important purpose of the GUI will be to produce a variety of RT displays of the activity of the PPS, such as:

Beam FWHM

Pointing RMS

Fudge Function

Feed Arm Modes

Wind

Thermal Model

The GUI will have commands to control which displays are visible and to select various modes for them.

Multiple instances of this X-window-based GUI can operate, so it will be possible for the operator and the observer to simultaneously have displays, with independent settings of modes. Perhaps some operational commands provided by the GUI will only be activated for the operator.

⁷TBD

⁸TBD

⁹TBD

¹⁰Remote operation capability is a natural consequence of this fact.

Chapter 3

Component Choices

3.1 Hardware Choice

I recommend that we plan to procure a multi-CPU SPARC in 1994. probably 4 CPUs at 75 MIPS each, ≥ 256 MB RAM, ≈ 20 GB disk, total system price \approx US\$100K. We need MIPS for decision-making, MFLOPs for linear algebra with a heavy emphasis on vector dot products, RAM for big matrices plus a big stream of data and derivatives and mass storage for archival data for offline analysis.

Code can be developed on single-CPU SPARC(s) of lower performance, can be debugged running with simulator at slower than RT or by simply reducing the bandwidth of the overall precision pointing servo.

3.2 OS Choice

Solaris 5.x, using multi-threaded-kernel, SVR4 semaphores and shared-memory features to do semi-hard RT [CH92].

3.3 Language Choice(s)

GNU C++ wherever possible, perhaps some Fortran for libraries. Will consider using Centerpoint (Saber C++) or equivalent (super gdb, probably with v.19 of GNU Emacs!?) as debugging environment.

Chapter 4

Development Plan

4.1 Staffing

two people, me and understudy. assume surface control already staffed. maybe add a programmer in 94 during implementation phase.

4.1.1 Understudy Concept

understudy to be permanent R&D person for pointing. should be physics-oriented rather than software-oriented. maybe would build simulator(s).

4.1.2 Mathematics & Engineering Support

I assume consulting support and possibly direct assistance by Fred Schwab (mathematics) and Chris Merrill (structural engineering).

4.2 Budget

Table 4.1 is a list of items that are likely to be procured, with rough estimates of prices and guesses as to which GBT account should fund them. This is *very* preliminary, intended to just get the discussion started. Several of the items in the list are described in the following subsections, others are mentioned elsewhere in the text.

4.2.1 Hardware Components

CPU not to be shared with other systems.

4.2.2 Software Components

NASTRAN Need license at least during software development.

PV-WAVE operator/developer interface

Item	\$K	Account	Notes
Inclinometers	6	PPS	
VME A-to-D	5	PPS	thermocouples
VME A-to-D	5	M&C	autocollimator
10 μ m Camera	\approx 200	PPS?	
frame grabber	3	PPS	digitize 10 μ m
weather station	5	PPS?	T, P, %
optical telescope	\approx 40	PPS	defer to 95
differential pressure	3	PPS	lift and drag
Mice!	50?	ClosedLoop	panel calibration
Computer	\approx 100	PPS	big SPARC
NASTRAN license	15?	PPS	check MSC terms
PV-WAVE license	3	PPS	NRAO site license?
Mathematica	2	PPS	use Schwab's at first
OODB	15?	PPS	use free Postgres?

Table 4.1: Budget for Precision Pointing

Mathematica procure tool for analytic work with vectors, matrices, derivatives. probably choose Mathematica because F.Schwab uses it.

Object-Oriented Database System We will accumulate a database of measurement and model history. It appears that an OODB would have definite advantages over a conventional RDMBS for this application. It might be possible to utilize the public domain "Postgres" package¹ from the Postgres group at Berkeley, but if not we will procure an OODB. We will use it to retain old measurements and old models, in order to permit flexible re-analysis of old data with evolving models. We must interpret old model solutions relative to new ones, fit to old models as though they are virtual measurement data. Probably this will utilize the classical concept of "normal points" to condense redundant measurement data.

4.3 Schedule for Precision Pointing Project

The duration of the Precision Pointing portion of the GBT construction project will be three years, from 1-Jan-93 through 31-Dec-95, consistent with the "final test" date 7-Dec-95 in a recent schedule by Hvatum [Hva92]. Table 4.2 lists the tasks to be done and guesses for their durations. I want to emphasize that this list is a first attempt which is mainly intended as a place-holder in the TIMELINE schedule until 1993 when the task list and estimated durations will be refined. Here are brief descriptions of some of the items:

¹anonFTP postgres.berkeley.edu: /pub/postgres-v3r1.tar.Z.

Task Name	Code	Weeks	Who	Predecessor	Successor
PRECISION POINTING	12				
DCW START	12.1		DCW	1-Jan-93	
INTERFACES	12.2		DCW		
Active Surface	12.2.1	3		12.1,4.3.7.5	
M&C	12.2.2				
Design	12.2.2.1	8		12.1,5.1.8	
Condon-style	12.2.2.2	16		12.2.2.1	
Rangefinders	12.2.3				
Design	12.2.3.1	4		12.1,3.18	
Implement	12.2.3.2	8		12.2.3.1	
Test	12.2.3.3	8		12.2.3.2	
ALIDADE TEST	12.3	12	DCW	12.1,2.8.2	
HIRE UNDERSTUDY	12.4	12	DCW	12.1	
SIMULATOR	12.5	26	Under	12.2.2.1,12.2.3.3,12.1	
NASTRAN TESTS	12.6	12	DCW	12.1	

Table 4.2: Schedule for Precision Pointing

Active-Surface Interface Test protocol for commanding actuators and returning LVDT readouts.

M&C Test protocol(s) for interfacing to M&C.

Rangefinders Develop protocol for commanding rangefinders and returning measurement data.

Pointing Corrections Decide on the specifications and mathematical form.

4.3.1 Phasing

attempt to deliver phase-3 plus phase-4 (dynamics!) at first light, but assure phase-2.

Note that because communication between PPS and other systems is via Internet, we could run tests of hardware and/or software using Charlottesville computers.

4.3.2 Contingency

phase-1 Condon-style pointing module should be built for M&C development and as fall-back plan in case of technical disappointment.

4.3.3 Issues and Possibilities

The following items are individual projects which may be appropriate to execute as a part of the overall PPS project. I have specified several of them in the preliminary schedule

tabulated above.

Build Experimental 4-Panel Testbed?

Consider building surface control program with mode tracking. use op amps with noise generator and oscillators to create drive signals for actuators under frame, and then fit RT models to track modes and generate drive signal for panel actuators. Should be able to demonstrate simultaneous solutions for tower mode vibrations and atmospheric fluctuations.

Build Alidade Test System?

Two or more laser rangefinders around the GBT at 100 meter radius with retroreflectors on the alidade would enable a series of experiments while construction is in progress in the Fall of 93. Could set up structural model of unloaded alidade and verify modal analysis, could verify thermal models, could measure track irregularities, etc.

Build a Simulator?

consider building a virtual M&C system which emulates dynamics of real telescope with environmental effects (temp and wind). consider whether this is of interest to M&C Group. consider building virtual laser system with environmental effects (index variations) and noise.

Build a Condon-Style Module?

insurance against technical problems, a contingency plan. would permit M&C project to operate it for testing during development phase.

Experiment With 140-Foot?

Several people have suggested that retroreflectors could be attached to the structure of the 140-Foot so that rangefinders could measure the behavior of this structure. I myself am currently unsure whether the experience gained from this experiment would be worth the software and systems integration effort that would be required. Further discussions of this idea are needed.

4.3.4 Technical TBDs

This is a list of technical questions which have arisen during my study of the PPS, and which are not yet resolved:

- subreflector/feed-arm/dish/alidade dynamical coupling? Especially potential coupling of torsional mode of alidade to azimuthal mode of feed arm at ≈ 0.7 Hz.
- are subreflector actuators spec-ed for 100% duty cycle at 1 Hz *forever*?

- RSi servo bandwidth properties? In particular, can bandwidths of subreflector actuator drives be increased above 1 Hz? Instead of specifying maximum bandwidth for full travel, could we instead specify maximum acceleration, which would imply a functional form for a limit on amplitude as a function of frequency? An informal memo by Jay Lockman [Loc92] appears to do just this, but it is unclear to me whether RSi has agreed to this. A good target would be upper bound of 3 Hz for servo cutoff for small amplitudes.
- Is RFI created by the panel actuators a problem? In particular, will it preclude panel motion while integrating?

Appendix A

Acknowledgements

I am grateful to a number of people who have talked with me about a variety of subjects while I have been preparing this memo:

Mike Balister methanol maser interferometer idea

Chuck Brockway autocollimator, inclinometer.

Mark Clark strategy, interface to M&C.

Jim Condon radio refraction, anomalous refraction, “outside-in” approach.

Geoff Croes project strategy, computing issues

Rick Fisher project strategy

Hein Hvatum schedule

Lee King thermal effects, vibrations.

Jay Lockman project strategy, philosophy.

Chris Merrill structural modelling, vibrations.

Dave Parker rangefinder details, acoustic thermometry.

John Payne everything!

Johan Schraml servos, M&C algorithms.

Fred Schwab geometry of laser rangefinders around dish, estimation of errors of solutions.

S. Srikanth beam computation from geometry, feed room/turret relationships.

Tim Weadon actuators, LVDTs, active surface interface. servos.

Bibliography

- [AUI89] AUI. The Green Bank Telescope: A radio telescope for the twenty-first century. Proposal to the national science foundation, Associated Universities, Inc., June 1989.
- [Bro90a] C. Brockway. GBT fine pointing. GBT Memo 38, National Radio Astronomy Observatory, March 1990. the autocollimator proposal.
- [Bro90b] C. Brockway. GBT lateral focussing. GBT Memo 33, National Radio Astronomy Observatory, February 1990. Discussion of pointing the GBT by tilting the subreflector.
- [CH92] Atri Chatterjee and Jim Herriot. Multithreading and real time. Solaris SunOS 5.0 White Paper, Sun Microsystems, Inc., July 1992. Broadcast as part of SunFlash bulletin 43.01 on 08-July-1992.
- [Con92] J. J. Condon. GBT pointing equations. GBT Memo 75, National Radio Astronomy Observatory, 1992. recommends GBT pointing coefficients be 2D Fourier series.
- [Cou91] C. E. Coulman. Tropospheric phenomena responsible for anomalous refraction at radio wavelengths. *Astron. Astrophys.*, 251:743–750, 1991.
- [D'A89] L. R. D'Addario. Active surface adjustment to nominal vs. nearby paraboloid. GBT Memo 20, National Radio Astronomy Observatory, October 1989.
- [Fin89] John W. Findlay. Notes on measuring distances. GBT Memo 24, National Radio Astronomy Observatory, November 1989. very similar to DCW concepts.
- [FvH72] J. W. Findlay and S. von Hoerner. A 65-meter telescope for millimeter wavelengths. Technical report, National Radio Astronomy Observatory, April 1972.
- [Hog89] D. E. Hogg. Some recent papers on anomalous seeing. GBT Memo 8, National Radio Astronomy Observatory, August 1989.
- [Hog90] D. E. Hogg. Atmospheric limitations on the GBT laser ranging system. GBT Memo 45, National Radio Astronomy Observatory, March 1990.

- [Hva92] Hein Hvatum. TIME LINE Gantt chart report. Interoffice memorandum, National Radio Astronomy Observatory, July 1992. Copy of main GBT schedule as of 13-July-92 (schedule file MAIN8).
- [IMS87] IMSL. *STAT/LIBRARY Users Manual*. IMSL, 1987. Version 1.0, April 1987. Fred Schwab has more recent versions of the IMSL library documents.
- [Jan91] C. Janes. VLA and VLBA antenna temperature measurements. VLA Test Memorandum 160, NRAO, Socorro, December 1991.
- [Kin92a] Lee King. private communication, 14 July 1992.
- [Kin92b] Lee King. Coefficient of expansion for steel. private Email, 15 July 1992. LKing says 'Unfortunately, I do not have info for cold temp range'.
- [Lam92a] James W. Lamb. Possibilities for wide-angle beam-switching. Millimeter Array Memo 86, NRAO, Tucson, June 1992.
- [Lam92b] James W. Lamb. Thermal considerations for mmA antennas. Millimeter Array Memo 83, NRAO, Tucson, May 1992. Good discussion of thermal effects on antennas.
- [Loc92] F. J. Lockman. Motions of the GBT. informal memo, 27 March 1992. One-page summary of motion specifications. Notable for specifying a subreflector *acceleration* but *not* a servo bandwidth cutoff!
- [Mer91] D. Christopher Merrill. Special design considerations for wind induced pointing errors in large unblocked aperture radio reflectors. GBT Memo 71, National Radio Astronomy Observatory, November 1991. results of pressure loadings applied to the NRAO NASTRAN model of the proof-of-concept elevation structure.
- [Mer92a] Chris Merrill. private communication, March(?) 1992.
- [Mer92b] Chris Merrill. NASTRAN timing formulæ. private Email, 15 July 1992.
- [MSC91] MSC. *MSC/NASTRAN Users Manual*. MacNeill-Schwindler Corporation, 1991.
- [Pay90] John Payne. Pointing and surface control of the GBT. GBT Memo 36, National Radio Astronomy Observatory, February 1990. the basic proposal.
- [Pay91] John Payne. Absolute/relative measurement. Interoffice memorandum, to bob hall, National Radio Astronomy Observatory, 11 December 1991. Proposes H-P laser for absolute calibration, argues that absolute ranging is needed for full pointing operation. Says "we could reasonably expect agreement between the instrument reading and the independent range calibration of around 120 μ ".

- [Pay92] J. M. Payne. Pointing the GBT. GBT Memo [draft, limited distribution], National Radio Astronomy Observatory, May 1992. Hardware point of view. Discusses pointing errors, instrumentation, present status and future plans, implementation, conclusions.
- [PP90] John Payne and David Parker. The laser ranging system for the GBT. GBT Memo 57, National Radio Astronomy Observatory, July 1990. Describes prototype, discusses group refractive index n_g .
- [PPB92] J. M. Payne, D. Parker, and R. Bradley. A rangefinder with fast multiple range capability. GBT Memo 73, National Radio Astronomy Observatory, 1992. (submitted to Rev. Sci. Instr.).
- [PPMR92] D. H. Parker, J. M. Payne, S. A. Massey, and S. L. Riley. The feasibility of acoustic thermometry for laser EDM temperature correction. GBT Memo 79, National Radio Astronomy Observatory, July 1992.
- [Sch90] Fred Schwab. Distortions of the antenna pattern due to surface-panel imperfections. GBT Memo 44, National Radio Astronomy Observatory, March 1990. This might be relevant for surface servo algorithm choice.
- [Sch91] Johann Schraml. Smooth tracking commands for periodic position updates. Memo [limited distribution], National Radio Astronomy Observatory, September 1991. Discusses acceleration profiles for optimum motion commands.
- [Sei89] George Seielstad. Notes from the GBT design workshop. GBT Memo 15, National Radio Astronomy Observatory, September 1989.
- [Sma62] W. M. Smart. *Textbook on Spherical Astronomy*. Cambridge University Press, 1962. 5th Edition.
- [Sri92] S. Srikanth. Correcting for gravity induced deformations. GBT Memo 78, National Radio Astronomy Observatory, May 1992. Deformations extracted from NASTRAN models.
- [Tho89] A. R. Thompson. Comments on 'active surface adjustment to nominal vs. nearby paraboloid'. GBT Memo 21, National Radio Astronomy Observatory, October 1989.
- [TMS86] A. Richard Thompson, James M. Moran, and George W. Swenson, Jr. *Interferometry and Synthesis in Radio Astronomy*. John Wiley & Sons, 1986. Chapter 13, "Propagation Effects", contains an excellent discussion of radio refraction.
- [vH90] Sebastian von Hoerner. Remarks about dynamics, atmosphere and summaries. GBT Memo 56, National Radio Astronomy Observatory, June 1990. Discusses lowest frequency ≈ 0.5 Hz and "homologous" scaling of geometry when laser distance scale is wrong.